



Biochar-plant interactions enhance nonbiochar carbon sequestration in a rice paddy soil

Zhiwei Liu^{1,2}, Wei Zhang ³, Ruiling Ma^{1,2}, Shixian Li^{1,2}, Kaiyue Song^{1,2}, Jufeng Zheng ^{1,2}✉, Yan Wang^{1,2}, Rongjun Bian^{1,2}, Xuhui Zhang^{1,2} & Genxing Pan^{1,2}

Soil amendment with biochar is being promoted as a promising strategy for carbon (C) stabilization and accrual, which are key to climate change mitigation. However, it remains elusive on how biochar addition influences nonbiochar C in soils and its mechanisms, especially in the presence of plants. Here we conducted a 365-day soil microcosm experiment with and without adding ¹³C-labeled biochar into topsoil to quantify changes in non-biochar C in the topsoil and subsoil in the presence or absence of rice plants and to determine the mechanisms by which biochar controls nonbiochar C accrual in the soil profile. The nonbiochar C content of topsoil was not affected by biochar addition in the absence of rice plants, but was significantly increased by 4.5% in the presence of rice plants, which could result from increases in the soil macroaggregate fraction, iron (Fe)-bound nonbiochar organic C content, and fungal biomass collectively. However, biochar amendment had no effect on the content of nonbiochar organic C in the subsoil. Overall, biochar-plant interactions drive more nonbiochar C sequestration in the topsoil, and the changes of nonbiochar C in planted soils following biochar addition should be quantified to better assess the soil C sequestration potential in agricultural lands.

¹Institute of Resource, Ecosystem and Environment of Agriculture, Nanjing Agricultural University, Nanjing, China. ²Jiangsu Collaborative Innovation Center for Solid Organic Waste Resource Utilization, Nanjing, China. ³Department of Plant, Soil and Microbial Sciences, Michigan State University, East Lansing, MI 48824, USA. ✉email: zhengjufeng@njau.edu.cn

Deployment of large-scale negative emission technologies is needed to curb average global warming to $<2^{\circ}\text{C}$ or possibly $<1.5^{\circ}\text{C}$ above preindustrial levels to meet the overarching climate goal of the Paris Agreement¹. Increasing carbon (C) storage in soils could be a promising strategy to mitigate climate change by sequestering atmospheric CO_2 into the soil C pool² while improving soil health and crop productivity^{3,4}. The urgency of climate change mitigation was highlighted at the 26th United Nations Framework Convention on Climate Change (UNFCCC) Conference of the Parties (COP26) in Glasgow in 2021⁵. Agriculture can contribute to substantial C sequestration by recycling organic materials into soil C pools, thereby enhancing food security and mitigating climate change^{6,7}.

Among the many soil organic amendments under consideration (e.g., fresh crop residues, manure, biosolids, and biochar), biochar has great potential for increasing soil C stocks^{8–11}. Biochar is produced by heating organic materials under oxygen-limited conditions (i.e., pyrolysis)¹², which results in more recalcitrant and persistent C-rich material¹³. In fact, biochar addition to soils could increase soil organic C (SOC) by an average of 39%, i.e., 6–8-fold of the SOC increase from conservation tillage and cover crops⁴. While the direct increase in SOC by biochar-C is well recognized, how biochar amendment influences other organic C (OC) forms (e.g., native SOC and plant litter) in soils, termed nonbiochar C, has long been debated. Previous studies showed either increase, decrease, or no effect of biochar amendment on the nonbiochar C^{14–17}, but most of these conclusions were drawn from laboratory incubation experiments without living plants^{18–21}. In soils with plants, the additional stabilization and accrual of nonbiochar C induced by biochar amendment could be substantial^{22,23}. Specifically, biochar amendment could profoundly influence the incorporation of plant and microbial biomass into SOC^{20,24,25}. However, the effect on nonbiochar C and its contribution to the total C pool in biochar-amended soils are not fully understood at present, especially in the soil profile. In fact, increased plant root biomass²⁶ or reduced positive priming of SOC mineralization by plants²⁴ in biochar-amended soils could lead to greater C sequestration potential. We recently found that biochar amendment increased photosynthetic C inputs by rice plants into subsurface soils by 14–20% using the ^{13}C pulse labeling method²⁷. Elucidating the effect of biochar amendment on soil C sequestration depends on distinguishing and quantifying changes in biochar-C and nonbiochar C (native SOC and plant-derived C) accumulation in the soil C pool in the presence of biochar and growing plants. However, many previous studies fell short of this aspect^{23,28,29}.

Indeed, various C forms in soils have a broad spectrum of stability against physical, chemical, and biological degradation. Increasing evidence indicates the crucial role of the SOC stabilization mechanism (physicochemical protection) in determining soil C turnover^{30,31}. For example, soil aggregates can offer physical protection of C from microbial degradation and thus critically impact microbial C cycling³². Adsorption or coprecipitation of newly accumulated C to soil minerals such as iron (Fe) oxides could facilitate C stabilization and accrual^{33,34}. Additionally, soil microorganisms regulate the formation soil aggregates^{35,36}. Meanwhile, soil microbial communities play a key role in regulating C turnover through the activities of extracellular enzymes^{37,38}, and fungi usually have a greater resource use efficiency than bacteria^{20,39}. Clearly, soil C sequestration by biochar amendment largely depends on the allocation and accumulation of organic matter in soils, which is driven by complex physical, chemical, and biological processes^{40–42}. A recent review highlights the significance of parallel evaluation of different mechanisms for understanding the role of biochar amendments

on soil C sequestration⁴³, but most experimental studies have addressed only one or two of these soil C sequestration mechanisms^{20,26,44}. Biochar amendment can simultaneously alter the physical, chemical, and biological properties of soils^{30,45}. However, there is insufficient experimental evidence to demonstrate how these mechanisms collectively drive C sequestration in soils with biochar addition.

We performed a 365-day microcosm experiment to elucidate the effect and controlling mechanisms of biochar amendment on C sequestration, especially the allocation and accumulation of nonbiochar C in soil profiles with growing rice plants. Field soil profiles were reconstructed in the microcosms using field-collected topsoil (0–15 cm) and subsoil (15–30 cm) samples from a rice paddy field. By tracking ^{13}C -labeled biochar-C applied to the topsoil in microcosms with or without growing rice plants, characterizing soil aggregates, quantifying Fe-bound OC, and determining microbial enzymatic activities and communities, we were able to determine whether biochar-plant interactions cause greater nonbiochar C accumulation and whether the increase is caused by enhanced plant and microbial biomass or physicochemical C protection. We hypothesized that (i) in the topsoil, biochar-plant interactions would drive more nonbiochar C sequestration by enhancing plant productivity, physicochemical protection, and biological functioning, and (ii) topsoil biochar amendment might not affect nonbiochar C accumulation in the subsoil after a 1-year period, but would limit subsoil microbial biomass and activity due to reduction of nutrient infiltration from the topsoil to the subsoil.

Here, we proposed a more holistic framework for soil C sequestration in biochar-amended soils. Briefly, biochar-plant interactions enhance physicochemical protection of plant-derived C via soil aggregates and chemical binding (Fe-bound OC), and increase fungal biomass (especially arbuscular mycorrhizal fungi, AMF), thereby increasing the accumulation of non-biochar C in the biochar-amended topsoil. In the subsoil underneath the biochar-amended topsoil, non-biochar C remains unchanged in one year, but microbial biomass and enzymatic activities are decreased with rice plants, probably due to nutrient limitation in the subsoil. Therefore, this study provides insights into the mechanisms of C sequestration in soils related to physical, chemical, and biological processes driven by biochar-plant interactions, and demonstrates that biochar amendment could enhance soil organic matter (SOM) accumulation.

Results

Rice shoot biomass. At the harvest of rice shoot on day 120, we found that biochar addition significantly increased rice shoot biomass by 23.3% ($p < 0.05$), with shoot biomass of 34.8 g pot^{-1} and 42.9 g pot^{-1} in the control and biochar treatments, respectively (Supplementary Fig. 1).

Soil chemical properties. Soil samples were collected at the end of 365-day microcosm experiment, we found that biochar addition significantly increased the total OC and total nitrogen (N) contents in the topsoil samples by 20.5–24.0% and 6.7–9.1%, respectively, compared with the biochar-free control treatment (Table 1). The nonbiochar C content in the topsoil samples with rice plants was increased by 4.5% ($1.0 \text{ g nonbiochar C kg}^{-1} \text{ soil}$; $p < 0.05$) by biochar addition from that of the control treatment, but remained unchanged in the absence of plants. The pH of the topsoil was also significantly increased by the addition of biochar. However, biochar addition to the topsoil did not affect the total OC and nonbiochar C contents of the subsoil, but decreased the total N content by 9.8% in the subsoil with plants. Furthermore, the contents of available N, available phosphorus (P), and

Table 1 Selected soil chemical properties of the topsoil and subsoil at the end of the 365-day microcosm experiment.

Treatment	Topsoil				Subsoil			
	Total OC (g kg ⁻¹)	Nonbiochar C (g kg ⁻¹)	Total N (g kg ⁻¹)	pH (H ₂ O)	Total OC (g kg ⁻¹)	Nonbiochar C (g kg ⁻¹)	Total N (g kg ⁻¹)	pH (H ₂ O)
Unplanted	21.2 ± 0.5	21.2 ± 0.5	2.31 ± 0.07	6.29 ± 0.03	12.8 ± 0.7	12.8 ± 0.7	1.49 ± 0.04	6.86 ± 0.05
Biochar	25.6 ± 0.5***	21.3 ± 0.4	2.47 ± 0.06*	6.49 ± 0.08*	13.2 ± 0.5	13.2 ± 0.5	1.45 ± 0.04	6.88 ± 0.05
Planted	22.4 ± 0.3	22.4 ± 0.3	2.34 ± 0.06	6.30 ± 0.06	14.5 ± 0.5	14.5 ± 0.5	1.79 ± 0.06	6.80 ± 0.06
Biochar	27.8 ± 0.7***	23.4 ± 0.5*	2.56 ± 0.05**	6.52 ± 0.07*	14.4 ± 0.7	14.3 ± 0.7	1.61 ± 0.03*	6.88 ± 0.07
Two-way ANOVA	***	ns	**	**	ns	ns	**	ns
Biochar	***	***	ns	ns	**	**	***	ns
Planted	ns	ns	ns	ns	ns	ns	*	ns
Biochar × planted								

Data are presented as the average of three replicates ± standard deviation. “*”, “**”, “***”, and “ns” indicate significance at $p < 0.05$, $p < 0.01$, $p < 0.001$, and no significance ($p > 0.05$), respectively.

available potassium (K) of topsoil were increased by biochar addition from that of the biochar-free control treatment, but biochar addition to the topsoil significantly decreased the available N and available P contents in the subsoil with plants (Supplementary Table 1).

Soil aggregates and nonbiochar C distribution in aggregates.

The effect of biochar on the distribution and stability of soil aggregates was examined using a wet-sieving method. We found that biochar addition to the topsoil increased the proportion of macroaggregates (250–2000 μm) by 18.4–24.2% but decreased the silt-clay fraction (<53 μm) by 7.1–16.6% (Fig. 1a), compared to the control treatment. In the subsoil, the distribution of aggregates was not significantly different between the biochar-free control and biochar-amended treatments with or without rice plants ($p > 0.05$; Fig. 1b). The mean weight diameter (MWD), a widely accepted indicator of soil aggregate stability, increased by 15.3–21.8% in the topsoil with biochar addition (Fig. 1c) but did not change in the subsoil underneath the biochar-amended topsoil (Fig. 1d).

Biochar addition changed the amount of nonbiochar C per unit aggregate mass (i.e., the nonbiochar C concentration). In the topsoil, biochar addition increased the nonbiochar C concentration in the macroaggregates by 8.6% ($p < 0.05$) in the presence of plants but decreased the nonbiochar C concentration in the microaggregates by 14.2% ($p < 0.01$) in the absence of plants (Supplementary Fig. 2a), compared to the control treatment. In the subsoil, the nonbiochar C concentration in the macroaggregates was 12.5% ($p < 0.05$) lower in the biochar-amended treatment than in the control treatment in the absence of plants, whereas there was no difference in the nonbiochar C distribution in soil aggregates between the control and biochar treatments in the presence of plants (Supplementary Fig. 2b). Furthermore, biochar addition changed the allocation and content of nonbiochar C in the topsoil samples. Specifically, the allocation of nonbiochar C increased in the macroaggregates (from 29.7% to 35.9% in the absence of plants; from 36.5% to 44.0% in the presence of plants) but decreased in the silt-clay fractions from 43.7% to 36.8% in the absence of plants in the biochar-amended soils (Fig. 2a). Additionally, the nonbiochar C content (i.e., nonbiochar C amount per unit dry mass of whole soil) in the macroaggregates increased by 21.5–28.6% in the biochar-amended soils than that in the biochar-free control treatments. However, for the subsoil, biochar addition to the topsoil did not affect the content and allocation of the nonbiochar C content within aggregates (Fig. 2b).

Fe-bound nonbiochar organic C content.

We explored the effect of biochar addition on the content of Fe-bound nonbiochar OC in the topsoil and subsoil at the end of 365-day microcosm experiment (Fig. 3). In the topsoil with plants, the Fe-bound nonbiochar OC content was increased by 9.7% with biochar addition from that of the biochar-free control treatment ($p < 0.05$). However, there was no significant difference in the Fe-bound nonbiochar OC content between the biochar and biochar-free control in the topsoil without plants ($p > 0.05$) and in the subsoil with or without plants ($p > 0.05$).

Soil enzyme activities and microbial community.

Two-way analysis of variance (ANOVA) results showed that biochar addition had a significant effect on soil enzyme activities in both topsoil and subsoil samples, except for β-xylosidase activity in the subsoil (Supplementary Table 2). Intriguingly, biochar addition to the topsoil increased the topsoil enzymatic activities by

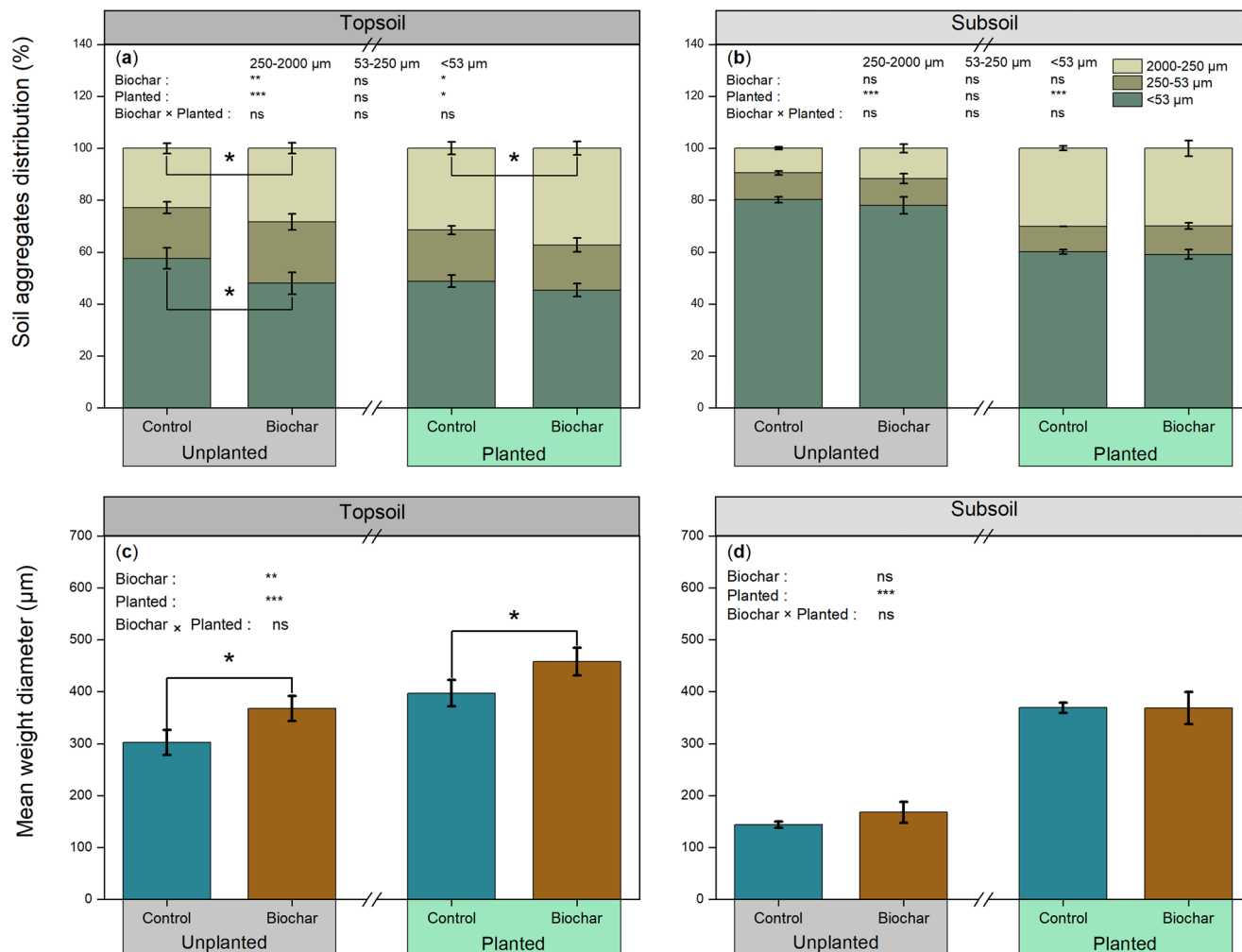


Fig. 1 Soil aggregate size distribution and mean weight diameter. Soil aggregate size distribution changes in the topsoil (a) and subsoil (b). Mean weight diameter changes in the topsoil (c) and subsoil (d). Data are presented as the average of three replicates \pm standard deviation. “*”, “**”, “***”, and “ns” indicate significance at $p < 0.05$, $p < 0.01$, $p < 0.001$, and no significance ($p > 0.05$), respectively.

15.1–39.9% but decreased the subsoil enzyme activities by 4.8–25.2%.

In the topsoil, biochar addition not only changed the microbial community structure (Supplementary Fig. 3a) but also increased the microbial biomass (Fig. 4a). Compared to the control treatment, biochar amendment increased all phospholipid fatty acids (PLFAs) by 10.1–19.8% in the absence of plants, and increased gram-negative bacteria (G⁻-bacteria), AMF, and saprotrophic fungi (SF) by 9.5%, 29.6%, and 16.8%, respectively, in the presence of plants. Furthermore, biochar addition increased the fungi/bacteria ratio of the topsoil in the presence of plants (Supplementary Fig. 4). However, biochar addition to the topsoil decreased the concentrations of the PLFAs compounds in the subsoil. Especially in the presence of plants, biochar addition decreased all PLFAs by 11.3–17.3% except for AMF in the subsoil (Fig. 4b).

Determinants of nonbiochar C sequestration in soils. To explore the potential mechanisms driving the observed variation in non-biochar OC among soils, we analyzed their relationships with several physical chemical, and biological predictors. The linear regression model showed that regardless of the soil depth, the nonbiochar C contents of the bulk soil were significantly positively correlated with the macroaggregate proportion (Supplementary

Fig. 5a), soil MWD (Supplementary Fig. 5b), and Fe-bound non-biochar OC content (Supplementary Fig. 5c). Structural equation model (SEM) analyses provided satisfactory goodness of fit using the χ^2 test and RMSEA in the topsoil (Fig. 5a) and the subsoil (Fig. 5c). The selected variables explained 97% and 70% of the variation in the nonbiochar C content of the bulk soil samples in the topsoil and the subsoil, respectively. In the topsoil, soil MWD and Fe-bound nonbiochar OC had direct and positive effects on the nonbiochar C content, with path coefficients of 0.62 and 0.35, respectively. However, plants and microorganisms affected the nonbiochar C content mainly through indirect pathways, with total path coefficients of 0.90 and 0.65, respectively (Fig. 5b). In the subsoil, the nonbiochar C content was dominantly and directly affected by soil MWD with a standardized direct effect of 0.66, while plants indirectly influenced the nonbiochar C content with a standardized indirect effect of 0.62 (Fig. 5d), likely by facilitating the formation of macroaggregates.

The variation partitioning analysis (VPA) for nonbiochar C further estimated the relative contributions of physical (MWD and macroaggregates), chemical (Fe-bound nonbiochar OC), and microbial (total PLFAs, AMF, fungi/bacteria ratio, and normalized enzyme activity) variables to the total variation of the optimized model. For the topsoil, the VPA results showed that physical, chemical, and microbial variables in total explained 82.9% of the variation in nonbiochar C, most of which (67.5%)

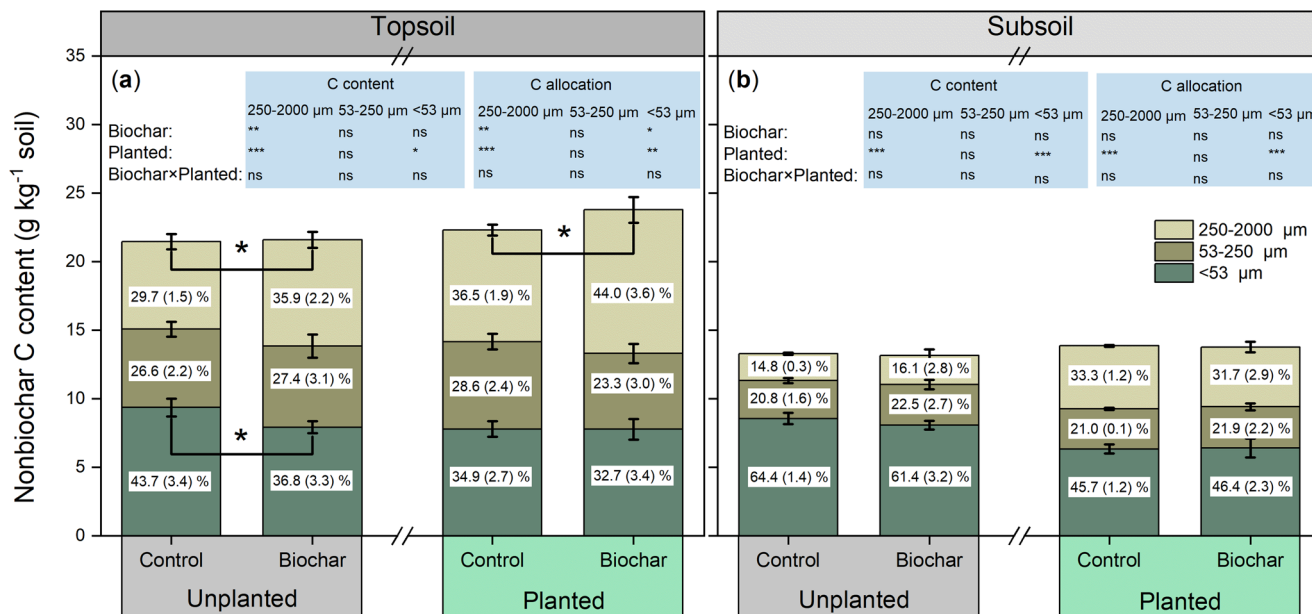


Fig. 2 The content and allocation of nonbiochar C within different aggregate size fractions. **a** in the topsoil and **b** in the subsoil. The values in the column graph represent the allocation ratio of nonbiochar C within different aggregate size fractions. Data are presented as the average of three replicates ± standard deviation. “*”, “**”, “***”, and “ns” indicate significance at $p < 0.05$, $p < 0.01$, $p < 0.001$, and no significance ($p > 0.05$), respectively.

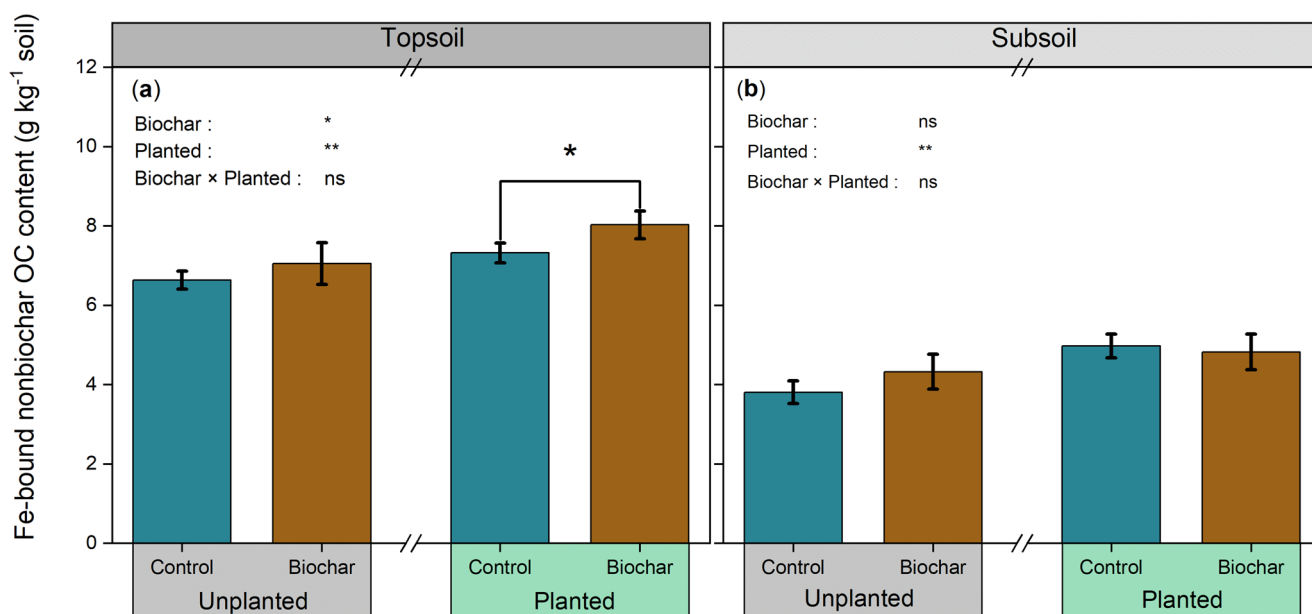


Fig. 3 Fe-bound nonbiochar OC content. **a** in the topsoil and **b** in the subsoil. Data are presented as the average of three replicates ± standard deviation. “*”, “***”, and “ns” indicate significance at $p < 0.05$, $p < 0.01$, and no significance ($p > 0.05$), respectively.

was due to their interactive effects (Fig. 6a). The individual effects of physical protection, chemical protection, and microbial properties explained 6.5%, 4.0%, and 5.4% of the total variation, respectively. In contrast to the topsoil, physical protection, chemical protection and microbial properties collectively accounted for 55.7% of the total variation in the nonbiochar C in the subsoil. However, the individual effect of physical protection explained a much higher proportion (12.5%) of the total variation than that of chemical protection (2.9%) and microbial properties (<0.1%) (Fig. 6b). These results demonstrated that the stabilization and accrual of nonbiochar C was primarily controlled by physical-chemical-microbial interactions in the topsoil and by aggregate protection in the subsoil.

Discussion

Our findings provide insight into the response of C in soils to biochar addition and the role of plant-biochar interactions in soil C sequestration. In this study, biochar addition increased the total OC content in the topsoil. Generally, increased soil C storage in biochar-amended soils mainly results from the higher persistence of biochar-C¹⁰. Nonetheless, emerging evidence highlights the positive role of plants in C accumulation with biochar amendment^{26,27,46}. We found that in addition to the accumulation of biochar-C, the nonbiochar C content increased in the topsoil with plants. However, the C accrual in the subsoil did not change significantly between the control and biochar treatments. Based on our results combining ¹³C isotopic analysis and

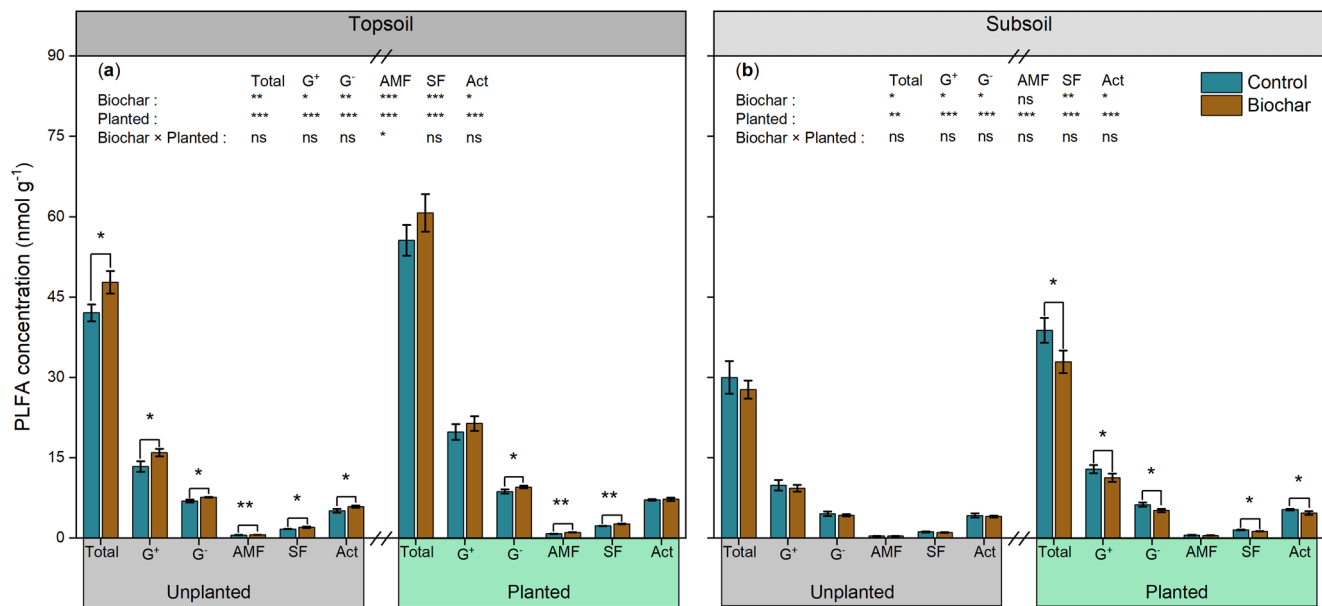


Fig. 4 Absolute concentration (nmol g⁻¹) of phospholipid fatty acids assigned to different microbial groups. a in the topsoil and **b** in the subsoil. PLFA, phospholipid fatty acid; G⁺, gram-positive bacteria; G⁻, gram-negative bacteria; AMF, arbuscular mycorrhizal fungi; SF, saprotrophic fungi; Act, actinomycetes. Data are presented as the average of three replicates ± standard deviation. “*”, “**”, “***”, and “ns” indicate significance at $p < 0.05$, $p < 0.01$, $p < 0.001$, and no significance ($p > 0.05$), respectively.

multivariate statistical analyses (SEM and VPA), this study provided empirical evidence that biochar addition changed C allocation and accumulation in the topsoil and the subsoil, which is characterized by a combination of physical protection, chemical protection, and biological processes (Fig. 7).

Soil C sequestration is closely related to the formation and stabilization of soil aggregates, which physically protect the SOM by forming a physical barrier between enzymes and microorganisms and their substrates³². In the topsoil, 34.4–37.9% and 47.0–50.9% of applied biochar-C was preserved in the macroaggregates and microaggregates, respectively (Supplementary Fig. 6a). Hence, the interactions between biochar particles and soil organic-mineral complexes may have promoted the formation of soil aggregates²⁶ and thus enhance the stability of soil aggregates (as characterized by MWD) in the topsoil. Biochar addition greatly enhanced the nonbiochar C concentration within macroaggregates of the topsoil in the presence of plants (Supplementary Fig. 2). Plant roots controlled C dynamics mainly through C input into the soil via rhizodeposition and root litter⁴⁷. In our recent study, we found that biochar addition fostered an increase in plant biomass during the rice growth stage, which may result in heightened photosynthetic C influx into the soil matrix²⁷. Moreover, labile and younger organic matter is more associated with the formation of macroaggregates, as fresh organic matter is a primary C source for microbial activity and thereby induces the binding of silt-clay-sized particles and microaggregates into macroaggregates⁴⁸. Therefore, during the phase of root decomposition, the enriched presence of fresh plant material (root litter) within the biochar-amended soil may be colonized by microbes and encrusted by primary soil particles through the binding action of microbial agents. As a cumulative effect, the amalgamation of these processes facilitated the formation of stable macroaggregates, concurrently elevating the C concentration⁴⁹. Simultaneously, greater light C would be physically protected in intra- and inter-macroaggregates in biochar-amended soil than in the biochar-free control treatment²³, resulting in increased C stored in the soil by enhancing the physical protection of organic matter in the macroaggregates⁵⁰.

The interaction of organic matter with the mineral phase, especially Fe oxides, is one of the main mechanisms that prevent microbial decomposition and thus stabilize C in the soil^{33,51}. Our results showed that biochar addition promoted the formation of Fe-bound nonbiochar OC in the topsoil, especially in the soils with rice plants. As shown by the SEM analysis, the C sequestration potential in the topsoil was directly determined by the Fe-bound nonbiochar OC. Biochar functions as a geobattery (electron shuttle) that facilitates microbial reduction of Fe(III) minerals to form Fe(II) under anaerobic conditions during the rice growth stage⁵². Subsequently, during the root decomposition phase, reoxidation of the soils could oxidize Fe(II) to Fe(III) and form Fe(III)-C complexes in the presence of dissolved organic matter by coprecipitation or adsorption of organic matter to Fe oxides, which directly contributes to C protection^{53–55}. Furthermore, the increase in root residues in biochar-amended soil may have promoted the complexation of Fe(III) with functional groups of C and the precipitation of these complexes⁵⁶. Consequently, biochar addition promoted the formation and stabilization of organic-mineral complexes and soil aggregates by bridging Fe(III) with newly organic matter and soil minerals, thus protecting C from microbial degradation²¹. However, the addition of biochar to the topsoil did not change the Fe-bound OC content in the subsoil compared to that of the control treatment, likely due to the negligible amount of biochar in the subsoil.

Soil microorganisms not only contribute to the formation of aggregates⁵⁷ but also participate in the decomposition and stabilization processes of SOM³⁸. During the rice plant growth stage, biochar as a physical growth matrix and nutrient source in combination with the rice root system might promote AMF colonization and development⁵⁸. The increase in AMF biomass in biochar-amended soils could improve soil aggregate stability because fungal hyphae are expected to promote the formation of macroaggregates by binding soil primary particles, small aggregates, and organic materials together^{59,60}, resulting in increased residence time of organic matter within macroaggregates. Biochar addition changed the microbial community structure in the topsoil (Supplementary Fig. 3), and the increased C:N ratio and

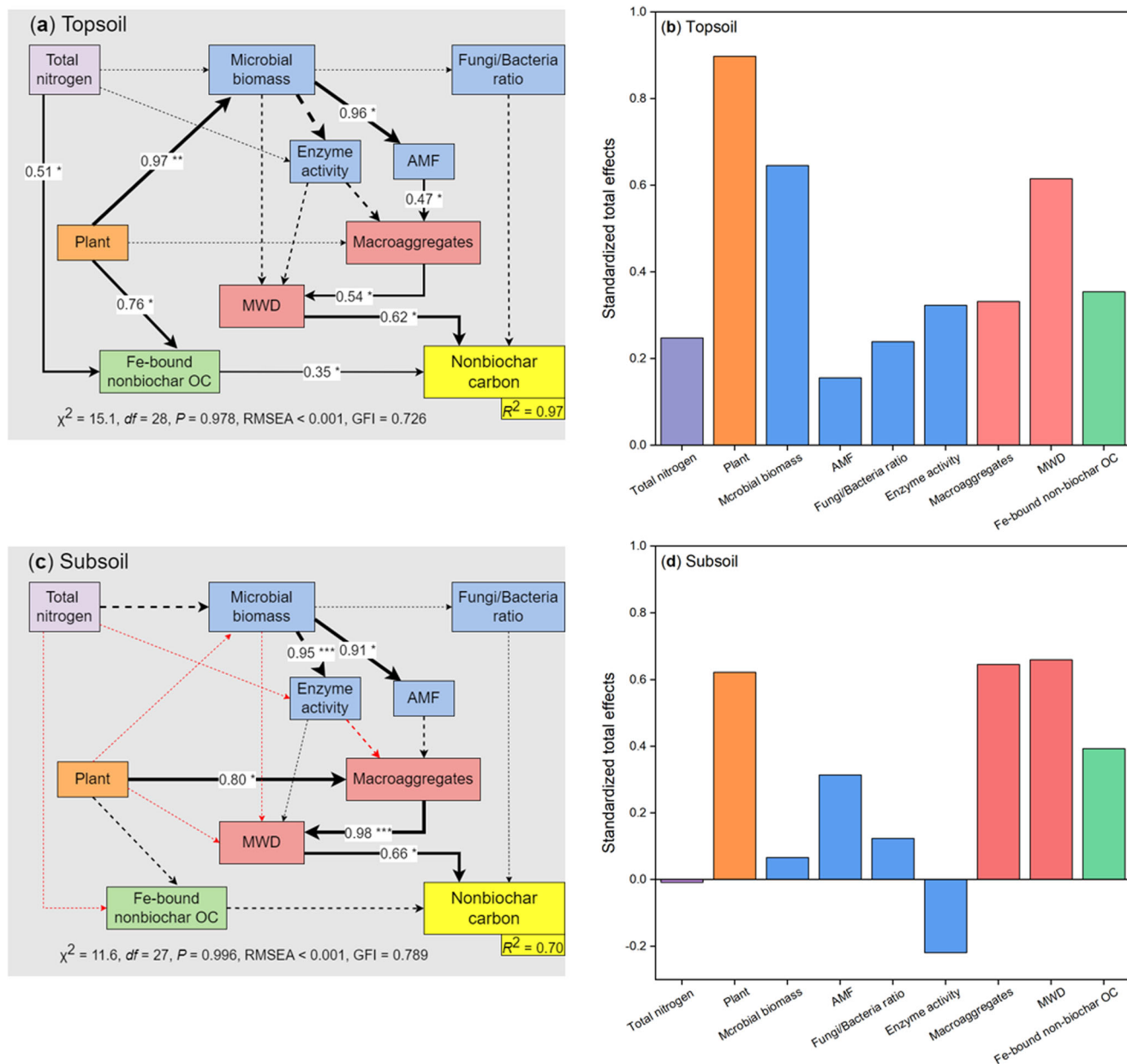


Fig. 5 Model of relationships between environmental variables and nonbiochar carbon content. Structural equation model (SEM) for quantifying the direct effects of physical, chemical, and biological factors on the nonbiochar C content of bulk soil in the topsoil (a) and subsoil (c), and the standardized total effects (indirect plus direct effects) in the topsoil (b) and subsoil (d) calculated by the SEM. “*”, “***”, and “****” indicate significance at $p < 0.05$, $p < 0.01$, and $p < 0.001$, respectively. Black and red arrows indicate positive and negative relationships, respectively. Solid and dotted arrows indicate significant and insignificant relationships, respectively. The arrow width is proportional to the strength of the relationship.

recalcitrant organic matter promoted fungal activity more than bacterial activity (Supplementary Fig. 4). Changes in microbial activity and composition in biochar-amended soil may alter microbial C use efficiency and C sequestration potential^{20,61}. It is acknowledged that on average, fungi generate more biomass C per unit of C metabolized than do bacteria, thus leading to a greater proportion of C being stored in fungal-dominated systems (high fungal-bacterial ratio) compared to bacterial-dominated systems⁶². In our previous study, we also found a greater microbial carbon C efficiency and C sequestration in fungal-dominated systems under biochar-amended soil²⁰. Therefore, during the root litter decomposition phase, higher C use efficiency in fungi-dominated (mainly saprotrophic fungi) system in the biochar-amended soil would cause more root-derived C

sequestration. Moreover, nutrient availability (e.g., N, P, and K) affects microbial growth and respiration because decomposer cells must maintain a balanced elemental composition, i.e., a balance of C and nutrient⁶³. The increase in nutrient availability in the topsoil with biochar addition would enhance the microbial C use efficiency. However, biochar addition to the topsoil decreased microbial biomass and enzyme activity in the subsoil, especially in the presence of plants. Biochar could enhance nutrient retention directly through chemical sorption and indirectly by improving soil aggregates^{64,65}, and thus reducing nutrient leaching into the deep soil^{66,67}. In this study, biochar addition increased the total N and available nutrient contents of the topsoil, whereas it may have limited the N and P leaching from the topsoil into the subsoil, especially in the presence of plants, thus

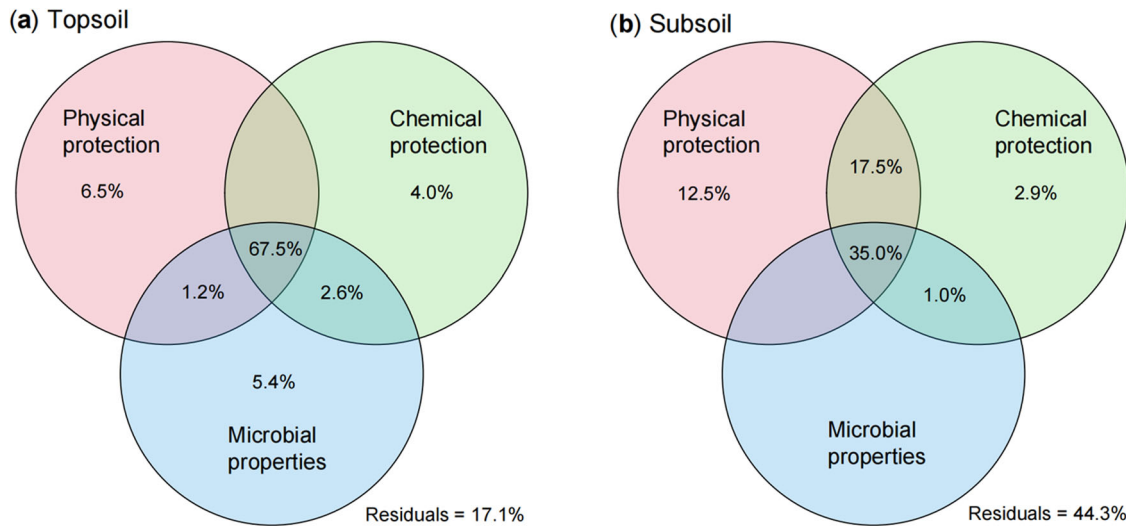


Fig. 6 Variation partitioning analysis for the variations in nonbiochar C content. **a** in the topsoil and **b** in the subsoil. Physical protection includes mean weight diameter and macroaggregates. Chemical protection refers to the Fe-bound nonbiochar OC content. Microbial properties include total phospholipid fatty acids and arbuscular mycorrhizal fungi concentrations, fungi/bacteria ratio, and normalized enzyme activity.

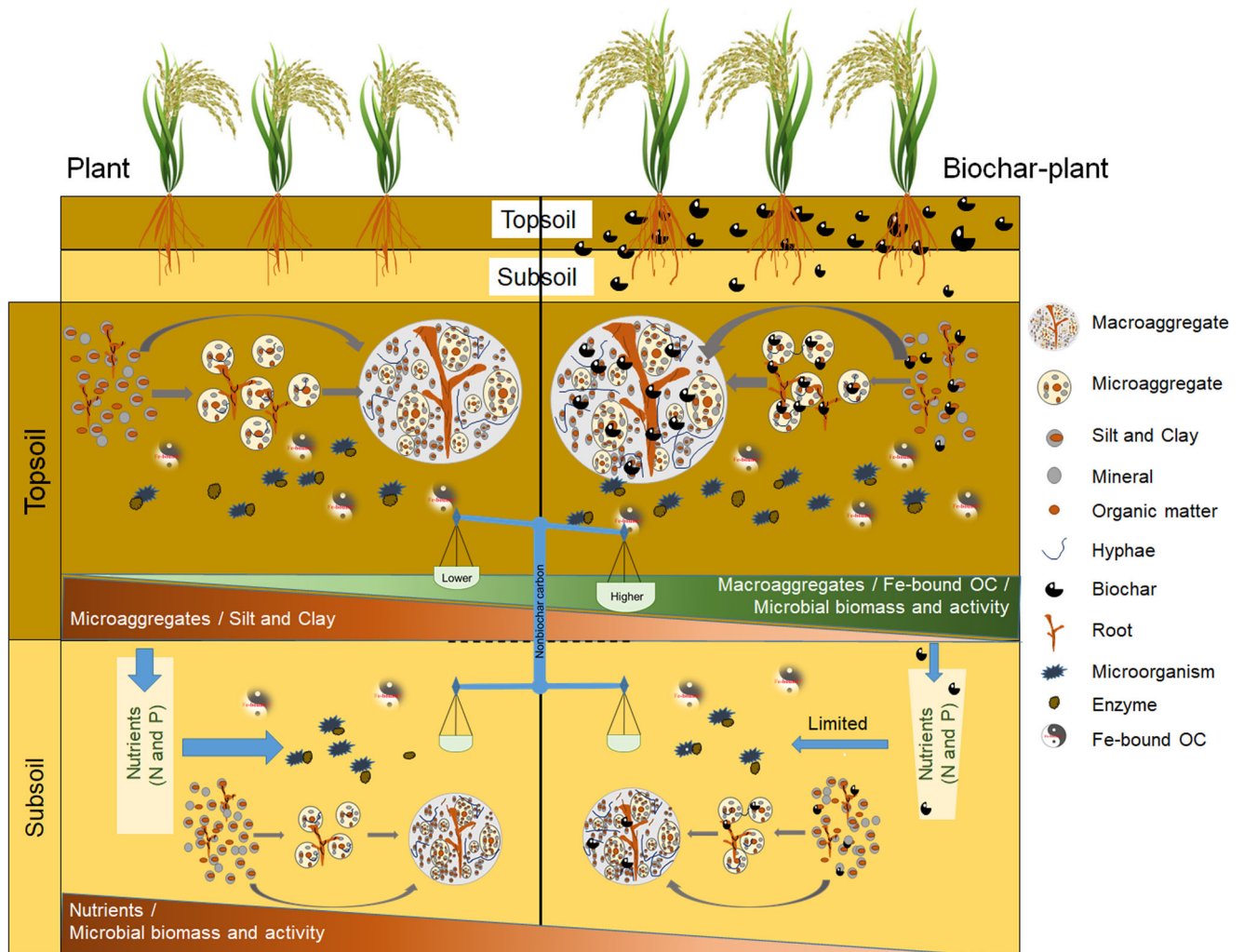


Fig. 7 Conceptual framework illustrating how biochar-plant interactions influence nonbiochar C sequestration and related physical, chemical, and microbial factors in the topsoil and subsoil. Biochar-plant interactions increased macroaggregates fraction, iron-bound organic C (Fe-bound OC) content, and microbial biomass and activity of the topsoil, resulting in increased nonbiochar C storage in the topsoil, whereas they decreased nutrient availability (available nitrogen and available phosphorus content) and microbial biomass and activity of the subsoil.

limiting the growth and activity of the subsoil microorganisms in the biochar-amended soil.

As C sequestration and greenhouse gas emission reduction in agriculture are becoming increasingly urgent, the use of biochar enriched with recalcitrant C as a soil amendment to increase soil C pools has been proposed as a global strategy to mitigate climate change^{10,68}. Many previous studies have mainly focused on the effect of biochar addition on greenhouse gas emission reductions and C sequestration potential related to the stability and persistence of biochar-C in soils^{10,13}, while overlooking the effect of biochar amendment on nonbiochar C stocks in soils, probably due to the inability to distinguish between C sources being biochar or nonbiochar (native SOC and plant-derived C)^{23,28}. Moreover, the high variation in field trials due to variability in climate, environment, and management factors and sampling uncertainty may overshadow the effect of biochar on nonbiochar C if its change in C is not dramatic. In this study, we found that the C sequestration potential of biochar soil amendment was attributed not only to the greater persistence of biochar-C but also to the increase in nonbiochar C in the rice paddy soils. Although the nonbiochar C content was only 4.5% (1.0 g non-biochar C kg⁻¹ soil) greater in the biochar-amended soil than in the biochar-free control treatment in the rice paddy, the non-biochar C storage in typical topsoil (0–15 cm depth) could be approximately increased by 1.7 t C ha⁻¹ based on a soil bulk density of 1.16 g cm⁻³ with only 1 year of biochar addition, which would be 2.8 times the level demanded by the “4 per 1000 Initiative” to offset emissions by 0.6 t C ha⁻¹ per year⁶⁹. Furthermore, the increase in soil C sequestration potential of biochar amendment could be lasting in future growing seasons following biochar application²³. We previously found that a higher C sequestration capacity for plant-derived C was still observed after three or even six years following biochar addition to the soil^{19,20}. Therefore, considering only the persistence of biochar-C while ignoring the accumulation of plant-derived C would underestimate the soil C sequestration potential offered by biochar amendment²⁶. Although there was no change in the nonbiochar C content of the subsoil after 1 year of biochar addition to the topsoil, we found a decrease in total N content, microbial biomass and enzyme activity, as well as changes in the microbial community in the biochar-amended subsoil. As biochar is applied over time, more biochar fragments are generated through physical breakdown, and these particles could percolate to the subsoil⁷⁰ and change the soil nutrient contents, which in turn would change the C storage in the subsoil⁷¹. Therefore, when assessing the C sequestration potential of biochar soil amendment, it is important to pay attention to the changes in C sequestration in the soil profile at longer time scales¹⁰. Furthermore, in this study, we only examined changes in the physical, chemical and microbial properties of soils at the end of 365-day microcosm experiment, which was suitable for exploring the effect of biochar amendment on nonbiochar C accrual in the soil profile and its mechanisms. However, nutrient evolution, plant biomass, physicochemical properties, and microbial endpoints might show very variable outcomes depending on sampling time^{25,27}. Thus, more comprehensive sampling within the period of the microcosm experiment could provide insight into how these variables vary and interrelate. In addition, in order to better distinguish the C dynamics in the 3-part systems including soil, biochar, as well as plants and their roots, we can apply dual ¹³C/¹⁴C isotopic labels to partition C sources in future studies⁷².

Conclusions

Our study used ¹³C-labeled biochar to determine the effect of topsoil biochar amendment on nonbiochar C allocation and

sequestration in the topsoil and the subsoil. Effects of biochar-plant interactions on C sequestration in the soil profile are the result of combined physical, chemical and microbial controls. In the topsoil, biochar addition promotes the formation of macroaggregates and Fe-bound OC, and improves microbial characteristics (abundance and activity), leading to higher nonbiochar C sequestration. In contrast, in the subsoil, biochar soil amendment did not change the C content but limited the microbial activity. These findings suggest that biochar-plant interactions and soil depth should be taken into account when assessing long-term C sequestration in soils amended with biochar. Future studies should be directed at studying other cropping systems and parameterizing such interactions into C cycle models to better predict the soil C sequestration potential of biochar amendment as a mitigation strategy for climate change.

Materials and methods

Soil samples and biochar preparation. The topsoil (0–15 cm depth) and subsoil (15–30 cm depth) samples for the microcosm experiment were collected from a rice paddy field in Jing-tang village (31°24'N, 119°41'E), Yixing Municipality, Jiangsu Province, China. This region is located on the southern edge of the Tai Lake Plain, and has a subtropical humid monsoon climate with a mean annual precipitation and temperature of 1177 mm and 15.7 °C, respectively. The soil was classified as a Hydroagric Stagnic Anthrosol⁷³. Fine roots and other visible plant residues in the soil samples were carefully removed, followed by air-drying, passing through a 2-mm sieve, and thorough homogenization before analysis of soil properties and the microcosm experiment. Selected physicochemical properties of the topsoil and subsoil samples were 21.8 g kg⁻¹ and 12.6 g kg⁻¹ SOC, 2.35 g kg⁻¹, and 1.50 g kg⁻¹ total N, 6.31 and 6.85 soil pH, 1.16 g cm⁻³ and 1.24 g cm⁻³ bulk density, and -28.45‰ and -27.02‰ δ¹³C, respectively.

The ¹³C-labeled biochar was produced from rice straw labeled with ¹³C using the ¹³CO₂ pulse-labeling procedure as described in our previous study²⁷. The ¹³C-labeled rice straws were first pulverized, passed through a 2-mm sieve, and then filled into closed steel crucibles. Next, the crucibles were heated in a muffle furnace at a rate of 5 °C min⁻¹ to 450 °C, which was maintained for 2 h before cooling to ambient temperature⁷⁴. The basic properties of the biochar were 462.5 g kg⁻¹ total C, 6.37 g kg⁻¹ total N, 4.63 g kg⁻¹ total P, 30.47 g kg⁻¹ total K, 30.12 cmol (+) kg⁻¹ cation exchange capacity, 9.43 pH and 1092 δ¹³C (‰).

Microcosm experiment. This microcosm experiment was conducted in a controlled environment chamber. The experimental treatments included: (1) biochar-free control treatment without rice plants; (2) biochar addition treatment (1% w/w) without rice plants; (3) biochar-free control treatment with rice plants; and (4) biochar addition treatment (1% w/w) with rice plants. Each treatment was replicated three times. Biochar was passed through a 1-mm sieve prior to incorporation into the soil samples. The subsoil and topsoil samples were filled to depths of 20–35 cm and 5–20 cm with polyvinyl chloride (PVC) tubes (35.0 cm in height, 15.0 cm in inner diameter, and 15.5 cm in outer diameter) at field bulk densities of 1.24 g cm⁻³ and 1.16 g cm⁻³, respectively. The 0–5 cm depth of the PVC tube was used to hold water during the rice growth stage. For the biochar addition treatments, the ¹³C-labeled biochar was thoroughly mixed with the topsoil sample at a rate of 1% (w/w) prior to packing into the PVC tube. For the treatments with rice plants, two 21-day-old rice seedlings (*Oryza sativa* L. cv., Changyou No.5) were transplanted into the soil. A schematic

setup is displayed in Supplementary Fig. 7. In the microcosms, 172 mg N kg⁻¹ (urea, equal to the local field application rate of 300 kg N ha⁻¹), 235 mg P kg⁻¹ (Ca(H₂PO₄)₂), and 235 mg K kg⁻¹ (KCl) on the basis of the topsoil mass were added as basal fertilizers. All microcosms were regularly irrigated with deionized water to maintain a water depth of 2–3 cm above the soil surface throughout the whole rice growth stage. During the rice growing period, the controlled-environment chamber was maintained at 32 °C/22 °C (day/night) with 12 h of supplemental lighting by LED light²⁷. For the planted treatments, the aboveground plant shoots were cut from the base of the stem at the rice maturity stage (total 120 days) and oven-dried, while the roots were retained in the soil. To stimulate the decomposition of plant roots in the soil, soil moisture was maintained at approximately 60% water holding capacity, and ambient temperature was controlled at 25 °C for 245 days, after the rice harvest.

Soil sampling. On Day 365, the topsoil and subsoil samples were retrieved from the microcosms. All fresh soil samples were handpicked to remove visible roots, homogenized, and then divided into three subsamples. One subsample was air-dried for chemical property analyses, one fresh subsample was used to determine the soil enzymatic activity and aggregate fractions, and the third subsample was freeze-dried for analysis of PLFAs.

Soil chemical analysis. The δ¹³C (‰) value, SOC, and total N of the air-dried soil samples were determined using a MAT253 isotope ratio mass spectrometer (IRMS) coupled with a FLASH 2000 elemental analyzer (Thermo Fisher Scientific, Waltham, MA, USA). Soil pH was measured with a soil/water ratio of 1:2.5 (w/v). Soil bulk density was determined using 100-cm³ soil cores and the gravimetric method. Available N (NH₄⁺ and NO₃⁻) was extracted from moist soil using 2-M KCl solution and analyzed on a continuous-flow autoanalyzer (Skalar San++, Holland). Available P was extracted using 0.5-M NaHCO₃ (pH 8.5) and analyzed using the molybdenum-antimony anti-spectrophotometric method. Available K was extracted with 1-M NH₄OAc and determined by a flame spectrophotometer (FP6410, INESA, China).

Determination of soil aggregate fractions. Soil aggregates were separated using a wet-sieving method according to Six, Paustian⁴⁸ with some modifications. Briefly, the fresh soil sample (100 g dry soil weight) was placed on top of a 2-mm sieve and submerged in deionized water for 10 min. The sequentially stacked sieves (2 mm, 250 μm, and 53 μm) were gently moved up and down 50 times with a distance of ~3 cm for 2 min. Soil mass on the 250-μm sieve and the 53-μm sieve was separately collected as macroaggregates (250–2000 μm) and microaggregates (53–250 μm), while those that passed through the 53-μm sieve were collected as the fine particle fraction (silt-clay). All aggregate-size fraction samples were dried at 60 °C for 72 h, weighed, and then ground to pass through a 0.15-mm sieve before analysis for δ¹³C (‰) value and C concentration of the aggregate size fraction.

Determination of Fe-bound organic C. Fe-bound OC of the bulk soil samples was extracted by the dithionite-citrate-bicarbonate (DCB) extraction method⁷⁵. Briefly, 0.50 g of a freeze-dried soil sample was mixed with 30 mL buffer solution (0.27 M trisodium citrate and 0.11 M sodium bicarbonate, pH 7.3) in a 50-mL polycarbonate centrifuge tube and heated to 80 °C in a water bath, followed by the addition of 0.5 g sodium

dithionite and maintenance at 80 °C for 15 min. To quantify the amount of C released from the soil sample during heating, the soil samples were extracted with sodium chloride (NaCl) at an equivalent ionic strength instead of trisodium citrate and sodium dithionite under the same conditions. Following both treatments, all samples were separated, and the supernatant was removed by centrifugation at 3000 × g for 10 min. Each soil sample was extracted three times using the buffer solution and then washed three times using deionized water. Finally, the residual soil samples were dried at 60 °C for 72 h and were then ground to pass through a 0.15-mm sieve before analyzing the δ¹³C (‰) value and C concentration of the DCB- or NaCl-extracted soil samples.

Enzyme activity analysis. Enzymatic activities of α-glucosidase, β-glucosidase, β-xylosidase and cellobiohydrolase were measured with modified universal buffer (MUB)-linked substrates through the fluorometric method⁷⁶. Briefly, each equivalent of 2.4 g dry mass of fresh soil was homogenized in 300 ml of buffer solution. Then, 200 μl of homogenized soil slurry and 50 μl of 200 μM MUB-linked substrate were dispensed into a black 96-well polystyrene plate. The fluorescence was measured at excitation wavelength of 365-nm and emission wavelength of 450-nm by a SpectroMaxM5 plate reader (Molecular Devices, USA).

Determination of microbial abundance. Microbial biomass and community composition were estimated by determination of PLFAs, which were extracted by a single-phase chloroform-methanol-citrate buffer mixture (1:2:0.8; pH = 4.0)⁷⁷. Briefly, 3.0 g of a freeze-dried bulk soil sample was extracted by a single-phase chloroform-methanol-citrate buffer mixture (1:2:0.8; pH = 4.0). Phospholipids were separated from neutral lipids and glycolipids on a solid phase extraction column (Supelco, Inc.) and then methylated by a mild alkaline methanolysis to form fatty acid methyl esters (FAMES). Methyl nonadecanoate fatty acid (19:0) was added as an internal standard. Finally, the FAME samples were dissolved in hexane and analyzed by gas chromatography (Agilent 7890 B, USA) coupled to a quadrupole mass selective detector (Agilent 5977 B, USA). The sums of PLFAs i14:0, i15:0, a15:0, i16:0, i17:0 and a17:0 were considered biomarkers for gram-positive bacteria (G⁺-bacteria); 16:1ω9c, 16:1ω7c, 17:1ω8c, cy17:0, 18:1ω7c, 18:1ω5c and cy19:0 for G⁻-bacteria; 16:1ω5c for AMF, 18:2ω6,9c and 18:1ω9c for SF; and 10Me16:0, 10Me17:0, and 10Me18:0 for actinomycetes. Meanwhile, the fungi/bacteria ratio was determined by dividing the sum of all fungal PLFAs markers (AMF and SF) by the sum of G⁺-bacteria, G⁻-bacteria, 15:00 and 17:00 PLFAs markers.

Data analyses. The nonbiochar C content was calculated by subtracting the ¹³C-biochar content from the total OC content.

The C content of each soil aggregate size fraction (g kg⁻¹ bulk soil) was calculated as follows:

$$\text{Content} = \frac{P_a \times c_a}{100} \quad (1)$$

where P_a and c_a are the proportion (%) and the C concentration (g kg⁻¹ aggregate) of the aggregate size fraction, respectively.

The δ¹³C values of biochar, soil and Fe-bound OC were expressed as δ values (‰) relative to the Pee Dee Belemnite standard, and then converted to atom (‰) using the following formula:

$$\text{Atom}(\%) = \frac{\left(\frac{\delta}{1000} + 1\right) \times 0.0111802}{\left(\frac{\delta}{1000} + 1\right) \times 0.0111802 + 1} \times 100 \quad (2)$$

The fractions of ^{13}C in soil C derived from biochar (f_{bs} , %) were calculated using the end-member mixing model⁷⁸ as follows:

$$f_{\text{bs}}(\%) = \frac{\text{Atom}_{\text{bs}} - \text{Atom}_{\text{cs}}}{\text{Atom}_{\text{biochar}} - \text{Atom}_{\text{cs}}} \times 100 \quad (3)$$

where Atom_{bs} , Atom_{cs} , and $\text{Atom}_{\text{biochar}}$ are the Atom (%) values of the biochar-amended soil, biochar-free control soil, and biochar samples, respectively. The ^{13}C of soil or Fe-bound OC derived from biochar is calculated by multiplying its fraction by the total OC content.

The Fe-bound OC content of the bulk soil sample was calculated based on the difference in the Fe-bound OC content between the NaCl-treated and DCB-treated samples, as follows:

$$\text{Fe-bound OC} = C_{\text{NaCl}} - C_{\text{DCB}} \quad (4)$$

where C_{NaCl} and C_{DCB} are the C contents of the soil residues after extraction with NaCl and DCB, respectively.

The $\delta^{13}\text{C}$ of Fe-bound OC ($\delta^{13}\text{C}_{\text{Fe-bound OC}}$) was calculated according to the isotopic mass balance⁷⁹, as follows:

$$\delta^{13}\text{C}_{\text{NaCl}} = \frac{\delta^{13}\text{C}_{\text{DCB}} \times (100 - f_{\text{Fe-bound OC}}) + \delta^{13}\text{C}_{\text{Fe-bound OC}} \times f_{\text{Fe-bound OC}}}{100} \quad (5)$$

$$\delta^{13}\text{C}_{\text{Fe-bound OC}} = \frac{\delta^{13}\text{C}_{\text{NaCl}} \times 100 - \delta^{13}\text{C}_{\text{DCB}} \times (100 - f_{\text{Fe-bound OC}})}{f_{\text{Fe-bound OC}}} \quad (6)$$

where $\delta^{13}\text{C}_{\text{NaCl}}$ and $\delta^{13}\text{C}_{\text{DCB}}$ are the C isotopic values of the soil residues after extraction with NaCl and DCB, respectively. $f_{\text{Fe-bound OC}}$ is the percentage of Fe-bound OC to total OC in the bulk soil sample.

The MWD of soil aggregates was calculated as follows²³:

$$\text{MWD} = \sum_{i=1}^3 P_i \times S_i \quad (7)$$

where P is the mass percentage of individual size fraction, S is the average diameter of the individual size fraction (μm), and i is a given soil aggregate fraction (i.e., macroaggregates, microaggregates, or silt-clay).

The individually measured enzyme activities were normalized to obtain an overall enzyme activity using the following equation²³:

$$x_i' = \frac{x_i}{\sum_{i=1}^{12} x_i} \quad (8)$$

where x_i is a single individual enzyme activity of a sample i (a total of 12 samples in the topsoil and subsoil), and x_i' is the normalized value of the individual enzyme activity of the sample. Subsequently, the arithmetic average of four measured enzyme activities was obtained as the normalized overall enzyme activity value for each sample.

The individual effects of biochar addition and rice planting, and their interactions on the measured parameters were analyzed by two-way ANOVA using JMP11.0 software (SAS Institute, USA). A two-sided t test was used to examine the effect of biochar addition on the measured parameters in the presence or absence of rice plants. A SEM was used to analyze the direct and indirect effects of physical, chemical, and biological variables on nonbiochar C in bulk soil samples using IBM-SPSS AMOS 23.0 software. The relative contributions of these unique and interaction effects of physical protection, chemical protection, and microbial properties on the variations in nonbiochar C content were determined by variation partitioning analyses (VPA) using the *varpart* function of the “vegan” package in R 4.1.2.

Reporting summary. Further information on research design is available in the Nature Portfolio Reporting Summary linked to this article.

Data availability

All source data for the figures presented in this manuscript and the Supplementary Information can be accessed at <https://doi.org/10.6084/m9.figshare.24464107.v1>.

Received: 8 March 2023; Accepted: 1 December 2023;

Published online: 21 December 2023

References

- Rogelj, J. et al. Paris Agreement climate proposals need a boost to keep warming well below 2 °C. *Nature* **534**, 631–639 (2016).
- Tautges, N. E. et al. Deep soil inventories reveal that impacts of cover crops and compost on soil carbon sequestration differ in surface and subsurface soils. *Glob. Chang. Biol.* **25**, 3753–3766 (2019).
- Bradford, M. A. et al. Soil carbon science for policy and practice. *Nat. Sustain.* **2**, 1070–1072 (2019).
- Bai, X. et al. Responses of soil carbon sequestration to climate-smart agriculture practices: a meta-analysis. *Glob. Chang. Biol.* **25**, 2591–2606 (2019).
- UNFCCC. Glasgow Climate Pact, November 2021, <https://unfccc.int/documents/310475> (2021).
- Chabbi, A. et al. Aligning agriculture and climate policy. *Nat. Clim. Chang.* **7**, 307–309 (2017).
- Lal, R. Soil carbon sequestration impacts on global climate change and food security. *Science* **304**, 1623–1627 (2004).
- Woolf, D., Amonette, J. E., Street-Perrott, F. A., Lehmann, J. & Joseph, S. Sustainable biochar to mitigate global climate change. *Nat. Commun.* **1**, 56 (2010).
- Lehmann, J. A handful of carbon. *Nature* **447**, 143–144 (2007).
- Lehmann, J. et al. Biochar in climate change mitigation. *Nat. Geosci.* **14**, 883–892 (2021).
- Elkhilifi, Z. et al. Potential role of biochar on capturing soil nutrients, carbon sequestration and managing environmental challenges: a review. *Sustainability* **15**, 2527 (2023).
- Sohi, S. P. Carbon storage with benefits. *Science* **338**, 1034–1035 (2012).
- Wang, J., Xiong, Z. & Kuzyakov, Y. Biochar stability in soil: meta-analysis of decomposition and priming effects. *GCB Bioenergy* **8**, 512–523 (2016).
- Zimmerman, A. R., Gao, B. & Ahn, M.-Y. Positive and negative carbon mineralization priming effects among a variety of biochar-amended soils. *Soil Biol. Biochem.* **43**, 1169–1179 (2011).
- Lu, W. et al. Biochar suppressed the decomposition of organic carbon in a cultivated sandy loam soil: a negative priming effect. *Soil Biol. Biochem.* **76**, 12–21 (2014).
- Luo, Y. et al. Priming effects in biochar enriched soils using a three-source-partitioning approach: ^{14}C labelling and ^{13}C natural abundance. *Soil Biol. Biochem.* **106**, 28–35 (2017).
- Chen, X. et al. Resistant soil carbon is more vulnerable to priming effect than active soil carbon. *Soil Biol. Biochem.* **168**, 108619 (2022).
- Keith, A., Singh, B. & Singh, B. P. Interactive priming of biochar and labile organic matter mineralization in a smectite-rich soil. *Environ. Sci. Technol.* **45**, 9611–9618 (2011).
- Liu, Z. et al. The responses of soil organic carbon mineralization and microbial communities to fresh and aged biochar soil amendments. *GCB Bioenergy* **11**, 1408–1420 (2019).
- Liu, Z. et al. Greater microbial carbon use efficiency and carbon sequestration in soils: amendment of biochar versus crop straws. *GCB Bioenergy* **12**, 1092–1103 (2020).
- Zheng, H., Wang, X., Luo, X., Wang, Z. & Xing, B. Biochar-induced negative carbon mineralization priming effects in a coastal wetland soil: Roles of soil aggregation and microbial modulation. *Sci. Total Environ.* **610–611**, 951–960 (2018).
- Chen, S. et al. Amendment of straw biochar increased molecular diversity and enhanced preservation of plant derived organic matter in extracted fractions of a rice paddy. *J. Environ. Manage.* **285**, 112104 (2021).
- Lu, H. et al. Legacy of soil health improvement with carbon increase following one time amendment of biochar in a paddy soil - a rice farm trial. *Geoderma* **376**, 114567 (2020).
- Whitman, T., Enders, A. & Lehmann, J. Pyrogenic carbon additions to soil counteract positive priming of soil carbon mineralization by plants. *Soil Biol. Biochem.* **73**, 33–41 (2014).

25. Weng, Z. et al. The accumulation of rhizodeposits in organo-mineral fractions promoted biochar-induced negative priming of native soil organic carbon in Ferralsol. *Soil Biol. Biochem.* **118**, 91–96 (2018).
26. Weng, Z. et al. Biochar built soil carbon over a decade by stabilizing rhizodeposits. *Nat. Clim. Chang.* **7**, 371–376 (2017).
27. Liu, Z. et al. Quantitative assessment of the effects of biochar amendment on photosynthetic carbon assimilation and dynamics in a rice-soil system. *New Phytol.* **232**, 1250–1258 (2021).
28. Liu, J. et al. Contrasting effects of straw and straw-derived biochar applications on soil carbon accumulation and nitrogen use efficiency in double-rice cropping systems. *Agric. Ecosyst. Environ.* **311**, 107286 (2021).
29. Blanco-Canqui, H., Laird, D. A., Heaton, E. A., Rathke, S. & Acharya, B. S. Soil carbon increased by twice the amount of biochar carbon applied after 6 years: field evidence of negative priming. *GCB Bioenergy* **12**, 240–251 (2020).
30. Weng, Z. H. et al. Microspectroscopic visualization of how biochar lifts the soil organic carbon ceiling. *Nat. Commun.* **13**, 5177 (2022).
31. Lehmann, J. & Kleber, M. The contentious nature of soil organic matter. *Nature* **528**, 60–68 (2015).
32. Six, J., Conant, R. T., Paul, E. A. & Paustian, K. Stabilization mechanisms of soil organic matter: Implications for C-saturation of soils. *Plant Soil* **241**, 155–176 (2002).
33. Torn, M. S., Trumbore, S. E., Chadwick, O. A., Vitousek, P. M. & Hendricks, D. M. Mineral control of soil organic carbon storage and turnover. *Nature* **389**, 170–173 (1997).
34. Curti, L. et al. Carboxyl-richness controls organic carbon preservation during coprecipitation with iron (oxyhydr)oxides in the natural environment. *Commun. Earth Environ.* **2**, 229 (2021).
35. Morris, E. K. et al. Visualizing the dynamics of soil aggregation as affected by arbuscular mycorrhizal fungi. *ISME J.* **13**, 1639–1646 (2019).
36. Fahad, S. et al. Agroforestry systems for soil health improvement and maintenance. *Sustainability* **14**, 14877 (2022).
37. Trivedi, P. et al. Microbial regulation of the soil carbon cycle: evidence from gene-enzyme relationships. *ISME J.* **10**, 2593–2604 (2016).
38. Sokol, N. W. et al. Life and death in the soil microbiome: how ecological processes influence biogeochemistry. *Nat. Rev. Microbiol.* **20**, 415–430 (2022).
39. Keiblinger, K. M. et al. The effect of resource quantity and resource stoichiometry on microbial carbon-use-efficiency. *FEMS Microbiol. Ecol.* **73**, 430–440 (2010).
40. Todd-Brown, K. E. O. et al. Causes of variation in soil carbon simulations from CIMP5 Earth system models and comparison with observations. *Biogeosciences* **10**, 1717–1736 (2013).
41. Luo, Y. et al. Toward more realistic projections of soil carbon dynamics by Earth system models. *Global Biogeochem. Cycles* **30**, 40–56 (2016).
42. Kyker-Snowman, E. et al. Increasing the spatial and temporal impact of ecological research: a roadmap for integrating a novel terrestrial process into an Earth system model. *Glob. Chang. Biol.* **28**, 665–684 (2022).
43. Joseph, S. et al. How biochar works, and when it doesn't: a review of mechanisms controlling soil and plant responses to biochar. *GCB Bioenergy* **13**, 1731–1764 (2021).
44. Bi, Y. et al. Structural and microbial evidence for different soil carbon sequestration after four-year successive biochar application in two different paddy soils. *Chemosphere* **254**, 126881 (2020).
45. Javed, M. A. et al. Positive and negative impacts of biochar on microbial diversity. In: *Sustainable Agriculture Reviews*. Fahad, S.; Danish, S.; Datta, R.; Saud, S.; Lichtfouse, E. (Eds.). Springer International Publishing: Cham. **61**, 311–330 (2023).
46. Pei, J. et al. Biochar-induced reductions in the rhizosphere priming effect are weaker under elevated CO₂. *Soil Biol. Biochem.* **142**, 107700 (2020).
47. Dijkstra, F. A., Zhu, B. & Cheng, W. Root effects on soil organic carbon: a double-edged sword. *New Phytol.* **230**, 60–65 (2021).
48. Six, J., Paustian, K., Elliott, E. T. & Combrink, C. Soil structure and organic matter: I. Distribution of aggregate-size classes and aggregate-associated carbon. *Soil Sci. Soc. Am. J.* **64**, 681–689 (2000).
49. Witzgall, K. et al. Particulate organic matter as a functional soil component for persistent soil organic carbon. *Nat. Commun.* **12**, 4115 (2021).
50. Nair, V. D. et al. Biochar in the agroecosystem-climate-change-sustainability nexus. *Front. Plant Sci.* **8**, 2051 (2017).
51. Dungait, J. A. J., Hopkins, D. W., Gregory, A. S. & Whitmore, A. P. Soil organic matter turnover is governed by accessibility not recalcitrance. *Glob. Chang. Biol.* **18**, 1781–1796 (2012).
52. Yang, Z. et al. A coupled function of biochar as geobattery and geconductor leads to stimulation of microbial Fe(III) reduction and methanogenesis in a paddy soil enrichment culture. *Soil Biol. Biochem.* **163**, 108446 (2021).
53. Chen, C., Hall, S. J., Coward, E. & Thompson, A. Iron-mediated organic matter decomposition in humid soils can counteract protection. *Nat. Commun.* **11**, 2255 (2020).
54. Giannetta, B. et al. The role of Fe(III) in soil organic matter stabilization in two size fractions having opposite features. *Sci. Total Environ.* **653**, 667–674 (2019).
55. Kleber, M. et al. Dynamic interactions at the mineral-organic matter interface. *Nat. Rev. Earth Env.* **2**, 402–421 (2021).
56. Wagai, R. & Mayer, L. M. Sorptive stabilization of organic matter in soils by hydrous iron oxides. *Geochim. Cosmochim. Acta* **71**, 25–35 (2007).
57. Six, J., Bossuyt, H., Degryze, S. & Denef, K. A history of research on the link between (micro)aggregates, soil biota, and soil organic matter dynamics. *Soil Tillage Res.* **79**, 7–31 (2004).
58. Hammer, E. C. et al. A mycorrhizal fungus grows on biochar and captures phosphorus from its surfaces. *Soil Biol. Biochem.* **77**, 252–260 (2014).
59. Lehmann, A., Zheng, W. & Rillig, M. C. Soil biota contributions to soil aggregation. *Nat. Ecol. Evol.* **1**, 1828–1835 (2017).
60. Rillig, M. C. & Mummey, D. L. Mycorrhizas and soil structure. *New Phytol.* **171**, 41–53 (2006).
61. Chen, L. et al. Competitive interaction with keystone taxa induced negative priming under biochar amendments. *Microbiome* **7**, 77 (2019).
62. Strickland, M. S. & Rousk, J. Considering fungal:bacterial dominance in soils – methods, controls, and ecosystem implications. *Soil Biol. Biochem.* **42**, 1385–1395 (2010).
63. Manzoni, S., Taylor, P., Richter, A., Porporato, A. & Agren, G. I. Environmental and stoichiometric controls on microbial carbon-use efficiency in soils. *New Phytol.* **196**, 79–91 (2012).
64. Laird, D., Fleming, P., Wang, B. Q., Horton, R. & Karlen, D. Biochar impact on nutrient leaching from a Midwestern agricultural soil. *Geoderma* **158**, 436–442 (2010).
65. Yoo, G., Kim, H., Chen, J. & Kim, Y. Effects of biochar addition on nitrogen leaching and soil structure following fertilizer application to rice paddy soil. *Soil Sci. Soc. Am. J.* **78**, 852–860 (2014).
66. Lehmann, J. et al. Australian climate-carbon cycle feedback reduced by soil black carbon. *Nat. Geosci.* **1**, 832–835 (2008).
67. DeLuca, T., Gundale, M., MacKenzie, M., Jones, D. Biochar effects on soil nutrient transformations. *Biochar Environ. Manage. Sci. Technol. Implement.* **2**, 421–454 (2015).
68. Smith, P. Soil carbon sequestration and biochar as negative emission technologies. *Glob. Chang. Biol.* **22**, 1315–1324 (2016).
69. Minasny, B. et al. Soil carbon 4 per mille. *Geoderma* **292**, 59–86 (2017).
70. Spokas, K. A. et al. Physical disintegration of biochar: an overlooked process. *Environ. Sci. Technol.* **1**, 326–332 (2014).
71. Luo, C., Yang, J., Chen, W. & Han, F. Effect of biochar on soil properties on the Loess Plateau: results from field experiments. *Geoderma* **369**, 114323 (2020).
72. Whitman, T., Singh, B. P., Zimmerman, A. R., Lehmann, J. & Joseph, S. Priming effects in biochar-amended soils: implications of biochar-soil organic matter interactions for carbon storage. *Biochar Environ. Manage. Sci. Technol. Implement.* **2**, 455–488 (2015).
73. Gong, Z. Anthrosols, classification of stagnic anthrosols. In: *Chinese soil taxonomy: theory approaches and application*. Beijing: Science Press (in Chinese) 160–165 (1999).
74. Bian, R. et al. Pyrolysis of crop residues in a mobile bench-scale pyrolyser: product characterization and environmental performance. *J. Anal. Appl. Pyrolysis* **119**, 52–59 (2016).
75. Lalonde, K., Mucci, A., Ouellet, A. & Gelinas, Y. Preservation of organic matter in sediments promoted by iron. *Nature* **483**, 198–200 (2012).
76. German, D. P. et al. Optimization of hydrolytic and oxidative enzyme methods for ecosystem studies. *Soil Biol. Biochem.* **43**, 1387–1397 (2011).
77. Frostegård, A. & Bååth, E. The use of phospholipid fatty acid analysis to estimate bacterial and fungal biomass in soil. *Biol. Fertil. Soils* **22**, 59–65 (1996).
78. Phillips, D. L., Newsome, S. D. & Gregg, J. W. Combining sources in stable isotope mixing models: alternative methods. *Oecologia* **144**, 520–527 (2005).
79. Wan, D. et al. Iron oxides selectively stabilize plant-derived polysaccharides and aliphatic compounds in agricultural soils. *Eur. J. Soil Sci.* **70**, 1153–1163 (2019).

Acknowledgements

This work was supported by the National Natural Science Foundation of China (41877097, 42277330, 42207351), the China Postdoctoral Science Foundation (2022M711654), and the Science and Technology Innovation Special Fund of Jiangsu Province for Carbon Dioxide Emission Peaking and Carbon Neutrality (BE2022423, BE2022304).

Author contributions

J.Z. and Z.L. conceived the research. Z.L., R.M., S.L., K.S. and Y.W. performed the sample collection and laboratory experiments analyses. Z.L. analyzed the data and wrote the first draft of the manuscript. W.Z., J.Z., R.B., X.Z. and G.P. provided comments on the manuscript.

Competing interests

The authors declare no competing interests.

Additional information

Supplementary information The online version contains supplementary material available at <https://doi.org/10.1038/s43247-023-01155-z>.

Correspondence and requests for materials should be addressed to Jufeng Zheng.

Peer review information *Communications Earth & Environment* thanks Alba Llovet and the other, anonymous, reviewer(s) for their contribution to the peer review of this work. Primary Handling Editors: Kate Buckeridge and Clare Davis. A peer review file is available.

Reprints and permission information is available at <http://www.nature.com/reprints>

Publisher's note Springer Nature remains neutral with regard to jurisdictional claims in published maps and institutional affiliations.



Open Access This article is licensed under a Creative Commons Attribution 4.0 International License, which permits use, sharing, adaptation, distribution and reproduction in any medium or format, as long as you give appropriate credit to the original author(s) and the source, provide a link to the Creative Commons licence, and indicate if changes were made. The images or other third party material in this article are included in the article's Creative Commons licence, unless indicated otherwise in a credit line to the material. If material is not included in the article's Creative Commons licence and your intended use is not permitted by statutory regulation or exceeds the permitted use, you will need to obtain permission directly from the copyright holder. To view a copy of this licence, visit <http://creativecommons.org/licenses/by/4.0/>.

© The Author(s) 2023